
Superconductivity in CaSn₃ single crystal with a AuCu₃-type structure

X. Luo^{1†}, D. F. Shao^{1†}, Q. L. Pei¹, J. Y. Song¹, L. Hu¹, Y. Y. Han², X. B. Zhu¹, W. H. Song¹,
W. J. Lu^{1*} and Y. P. Sun^{1,2,3*}

¹ Key Laboratory of Materials Physics, Institute of Solid State Physics, Chinese Academy of Sciences, Hefei, 230031, China

² High Magnetic Field Laboratory, Chinese Academy of Sciences, Hefei, 230031, China

³ Collaborative Innovation Center of Advanced Microstructures, Nanjing University, Nanjing, 210093, China

Abstract

We report the superconductivity of the CaSn₃ single crystal with a AuCu₃-type structure, namely cubic space group $P_{m\bar{3}m}$. The superconducting transition temperature $T_C=4.2$ K is determined by the magnetic susceptibility, electrical resistivity, and heat capacity measurements. The magnetization versus magnetic field (M - H) curve at low temperatures shows the typical-II superconducting behavior. The estimated lower and upper critical fields are about 125 Oe and 1.79 T, respectively. The penetration depth $\lambda(0)$ and coherence length $\xi(0)$ are calculated to be approximately 1147 nm and 136 nm by the Ginzburg-Landau equations. The estimated Sommerfeld coefficient of the normal state γ_N is about 2.9 mJ/mol K². $\Delta C/\gamma_N T_C = 1.13$ and $\lambda_{ep} = 0.65$ suggest that CaSn₃ single crystal is a weakly coupled superconductor. Electronic band structure calculations show a complex multi-sheet Fermi surface formed by three bands and a low density of states (DOS) at the Fermi level, which is consistent with the experimental results. Based on the analysis of electron phonon coupling of AX₃ compounds (A=Ca, La, and Y; X=Sn and Pb), we theoretically proposed a way to increase T_C in the system.

[†]X. Luo and D. F. Shao contributed equally to this work.

*Author to whom correspondence should be addressed. Electronic mail: wjlu@issp.ac.cn and yypsun@issp.ac.cn

I. Introduction

LnM_3 ($\text{Ln}=\text{Y}$ and rare-earth elements, $\text{M}=\text{Pb}$, Tl , In , Ga , and Sn) compounds crystallized in a cubic AuCu_3 -type structure have attracted much attention due to their interesting physical properties, such as superconductivity, heavy fermion behavior, quantum critical point and so on.[1,2] LnSn_3 compounds are particularly intriguing as they are found to have relatively higher superconducting transition temperature T_C . For instance, the T_C of LaSn_3 is 6.5 K and that of YSn_3 is 7.0 K, whereas Pb , Tl , In , and Ga related compounds have lower T_C . [3-6] On the other hand, some LnSn_3 compounds show additional interesting physical phenomena. For example, PrSn_3 has been reported to be a heavy fermion compound with an antiferromagnetic order at $T_N=8.6$ K and CeSn_3 is categorized as a dense Kondo compound with valence fluctuation. [7,8] However, the isostructural ASn_3 ($\text{A}=\text{alkaline earth metal}$) compounds are seldomly explored; the ion-ratio mismatch between the alkaline earth metal ions and Sn one, it is difficult to crystallize into a AuCu_3 -type structure. For instance, BaSn_3 and SrSn_3 with superconducting transition temperature $T_C=2.4$ K and 5.4 K distort into hexagonal and rhombohedra structures, respectively. [9,10] Different from the distorted BaSn_3 and SrSn_3 compounds, CaSn_3 with smaller Ca ion can be crystalized into a AuCu_3 -type structure and it has the same structure with CaPb_3 and CaTl_3 superconductors. [11-13] Although the polycrystalline CaSn_3 was synthesized thirty years ago, the physical properties of CaSn_3 have been rarely reported because the CaSn_3 is a decomposition product of highly air-sensitive. To the best of our knowledge, the de Has-van Alphen effect has only been observed in polycrystalline CaSn_3 powder. [11] In order to get a deeper insight into the physical properties of CaSn_3 single crystal, further research is needed.

Herein, we have successfully grown the bulk single crystals of CaSn_3 for the first time and discovered that it shows superconductivity with $T_C=4.2$ K. We have performed electrical resistivity, magnetic susceptibility, and heat capacity measurements to determine the superconducting parameters of CaSn_3 single crystal. Furthermore, electronic band structure calculations suggest a complex, multi-sheet Fermi surface formed by three bands. The calculated low density of states (DOS) at the Fermi level is almost consistent with the value derived from the small electron specific coefficient measured. Finally, based on the analysis of electron phonon coupling (EPC) of AX_3 compounds ($\text{A}=\text{Ca}$, La , and Y ; $\text{X}=\text{Sn}$ and Pb), we theoretically proposed a way to increase T_C in the

system.

II. Experimental details

Single crystalline specimens of CaSn_3 were prepared through Sn-self flux. Ca pieces (99.99 %, Alfa Aesar) and Sn powders (99.99 %, Alfa Aesar) with mole ratio 1:28 were weighted and loaded into a 2 mL alumina crucible, which was sealed in an evacuated quartz tube. All were done in an Ar-filled glove box. The sealed quartz tubes were slowly heated to 800 °C for 24 hours, and dwelled for 24 hours, then slowly cooled down to 270 °C with 2 °C/h. Finally, the quartz tubes were inverted and quickly spun into a centrifuge to remove the excess Sn flux. More detail can be found in the Supporting information. Rectangular single crystals with shining surface were observed. The size was about $1.5 \times 1.5 \times 1 \text{ mm}^3$. The single crystals were air-sensitive and thus they were kept inside the glove box until characterization. Such handling was necessary to avoid decomposition. Powder X-ray diffraction (XRD) patterns were taken with Cu $K_{\alpha 1}$ radiation ($\lambda=0.15406 \text{ nm}$) using a PANalytical X'pert diffractometer at room temperature. Heat capacity and electrical transport properties were measured using the Quantum Design physical properties measurement system (PPMS-9T) and magnetic properties were performed by the magnetic property measurement system (MPMS-XL5). The electrical transport measurements were performed by a four-probe method to eliminate the contact resistance. The measurement of specific heat was carried out by a heat-pulse relaxation method on PPMS-9T. Electronic structures were obtained from first-principles density functional theory in the generalized gradient approximation (GGA) according to the Perdew-Burke-Ernzerhof.[14] The QUANTUM-ESPRESSO package was used with ultrasoft pseudopotentials generated by Garrity, Bennett, Rabe, and Vanderbilt (GBRV).[15,16] The energy cut off for the plane-wave basis set is 40 Ry. Brillouin zone sampling is performed on the Monkhorst-Pack (MP) mesh of $16 \times 16 \times 16$. [17]

III. Results and Discussion

CaSn_3 shows a cubic structure with space group $P_{m\bar{3}m}$, as present in Fig. 1 (a). Ca ions set in the corner and six Sn ions are octahedrally coordinated without atoms inside. Figure 1(b) shows the powder X-ray of CaSn_3 single crystals which were ground in a glove box. The sample powder was sealed by Kapton film during the measurement to protect it from oxidation. As shown in Fig. 1 (b),

it presents a cubic structure with little Sn-flux impurity, which may be due to the decomposition of CaSn₃ powder during the grinding and data collection. The high intensity in the low degree zone is the background from the Kapton film. The lattice constant a calculated from indexes is about 4.742 Å, which matches well with the previously reported value.[11]

Figure 1 (c) shows the resistivity dependence of temperature of CaSn₃ single crystal from 300 K to 2 K. The electrical resistivity data show a metallic behavior ($\frac{d\rho}{dT} > 0$) with the large residual resistivity ratio (RRR): $\frac{\rho_{300K}}{\rho_{5K}} \sim 73$, which indicates the CaSn₃ single crystal is of high quality. A clear superconducting transition can be observed at 4.2 K. We applied the Fermi-liquid model $\rho(T) = \rho_0 + AT^2$, where ρ_0 and A are the residual resistivity and a constant, respectively, to the curve below 20 K as shown in the inset of Fig. 1 (c). The model analysis yielded the residual resistivity ρ_0 of 1.3 $\mu\Omega cm$ and the coefficient A of 0.00227 $\mu\Omega cm/K^2$, indicating Fermi-liquid-like behavior for CaSn₃ single crystal.

The ρ versus T curve of CaSn₃ single crystal was further analyzed over the whole temperature range by the Bloch-Grüneisen-Mott (BGM) model, which is expressed as[18]

$$\rho_{BGM}(T) = \rho_0 + 4\mathcal{R}T \left(\frac{T}{\Theta_R}\right)^4 \int_0^{\Theta_R/T} \frac{x^5}{(e^x-1)(1-e^{-x})} dx \quad , \quad (1)$$

where ρ_0 is the residual resistivity and \mathcal{R} is a constant. The second term represents contributions from the electron-phonon interaction and Θ_R is the Debye temperature.[19] Least-squares fit of the $\rho(T)$ data by Eqs. (1) for 5 K $\leq T \leq$ 300 K is shown in Fig.1 (c). Fig. 1S shows the fitting data at low temperature. The parameters were estimated to $\rho_0=1.5 \mu\Omega cm$, $\mathcal{R}=0.17 \mu\Omega cm/K$, and $\Theta_R=211$ K.

Figure 1 (d) presents the temperature dependence of magnetization with the zero-field and field cooling (ZFC and FC) modes under applied magnetic field 10 Oe. The bulk superconducting transition temperature $T_C=4.2$ K can be clearly seen in the left inset of Fig. 1 (d), which is consistent with the resistivity result. The magnetization as a function of magnetic field at 2.5 K is shown in the right inset of Fig. 1 (d). The clear hysteresis is observed, which indicates a typical type-II superconducting behavior of CaSn₃ single crystal. The little element Sn may be left on the CaSn₃ single crystal surface, we compared the magnetization as a function of magnetic field curves of CaSn₃ single crystal and element Sn at $T=3.6$ K, as shown in Fig. 2S. The CaSn₃ single crystal shows

a typical type-II superconductor, which is different from the element Sn with type-I superconducting behavior.

In order to gain further insights into the superconducting state, the magneto-resistivity and the magnetic field dependence of magnetization at various temperatures were performed. Figure 2 (a) shows the resistivity under different magnetic fields. T_C at different magnetic field is determined at a 50 % decrease from the normal-state resistivity value, and transition width is taken as the temperature interval between 10% and 90 % of the transition. Figure 2 (b) presents the H_{C2} - T phase diagram of the superconducting state of CaSn_3 single crystal. We estimate the upper critical field, $H_{C2}(0)$, from the Werthamer-Helfand-Hobenberg (WHH) expression[20]

$$\mu_0 H_{C2}(0) = -0.693(dH_{C2}/dT)_{T=T_C} T_C . \quad (2)$$

A nearly linear relationship is obtained in the measured temperature range, which leads to a $\mu_0 H_{C2}(0)$ value of 1.79 T. The value of $\mu_0 H_{C2}(0)$ is lower than the Pauli-limiting field

$$\mu_0 H^{Pauli} = 1.24 k_B T_C / \mu_B . \quad (3)$$

Expected within the same weak-coupling BCS theory, it is about 7.6 T for $T_C=4.2$ K.[21] The empirical formula:

$$H_{C2}(T) = H_{C2}(0) \left[1 - \left(\frac{T}{T_C} \right)^2 \right]^{\frac{3}{2}} , \quad (4)$$

which is usually used to calculate the upper critical field for a variety of intermetallic and oxide superconductors.[22,23] The value of upper field is about $\mu_0 H_{C2}(0)=1.86$ T, which agrees well with the $\mu_0 H_{C2}(0)$ obtained from WHH method. The upper critical field value $\mu_0 H_{C2}(0)$ can be used to estimate the Ginzburg-Landau (GL) coherence length $\xi(0) = \sqrt{\frac{\Phi_0}{2\pi H_{C2}(0)}} = 136 \text{ \AA}$, where $\Phi_0=hc/2e$ is the flux quantum.

Figure 2 (c) shows the magnetization as a function of magnetic field at different temperatures below T_C . $\mu_0 H_{C1}(0)$ as a function of T is present in the Fig. 2 (d). The lower critical field is analyzed using the equation:

$$H_{C1}(T) = H_{C1}(0) \left[1 - \left(\frac{T}{T_C} \right)^2 \right] . \quad (5)$$

The value of $\mu_0 H_{C1}(0)$ is about 125 Oe. In addition, we may estimate the Ginzburg-Landau (GL) parameter $\kappa = 1/\sqrt{2}[H_{C2}(0)/H_C(0)] \sim 8.4$, where the thermodynamic critical field

$H_C(0)=(H_{C1}(0)H_{C2}(0))^{1/2}\sim 0.15$ T, and the magnetic penetration depth $\lambda(0)$ is found to be 1147 Å from $\lambda(0)=\kappa\xi(0)$. [24]

The temperature dependence of specific heat C_P also presents more information about the superconducting properties. Figure 3 (a) shows the temperature dependence of the heat capacity C_P of CaSn₃ single crystal at $H=0$ and 5 T. At $H=0$ T, the specific heat data show the bulk superconducting feature as indicated by the clear jump of C_P around T_C . At $H=5$ T, the specific heat jump of superconductivity in CaSn₃ single crystal is completely suppressed. C_P/T varies almost linearly with T^2 above T_C . The Sommerfeld constant γ_N is obtained from the fit $C_P/T=\gamma_N+\beta T^2$ (γ_N and β are T -independent coefficients), where γ_N is the normal-state electronic contribution and β is the lattice contribution to the specific heat. The fitting results yield $\gamma_N=2.9$ mJ/mol K² and $\beta=1.45$ mJ/mol K⁴. The Debye temperature Θ_D can be determined from the coefficient of the T^3 term $\beta=N(12/5)\pi^4 R\Theta_D^{-3}$, where $R=8.314$ J/mol K and $N=4$ for CaSn₃ single crystal. Θ_D is about 175 K, which is little lower than that of YSn₃. [6] The Debye temperature Θ_D obtained from the low temperature heat capacity C_P was slightly lower than the Debye temperature $\Theta_R=211$ K derived from the resistivity data because the Θ_R obtained from the resistivity was averaged over the whole temperature range. It is known that the ratio $\Delta C_P/\gamma_N T_C$ can be used to estimate the coupling strength. [25] As shown in the inset of Fig. 3, $\Delta C_P/\gamma_N T_C$ of CaSn₃ single crystal from the C_P data is about 1.13, which is slightly lower than the expected BCS value with $\Delta C_P/\gamma_N T_C \sim 1.43$ for superconductors within the weak-coupling limit. This suggests that the CaSn₃ single crystal is a weakly coupled superconductor. An estimation of the strength of the EPC can be derived from the McMillan formula: [26,27]

$$\lambda_{ep} = \frac{\mu^* \ln\left(\frac{1.45T_C}{\Theta_D}\right) - 1.04}{1.04 + \ln\left(\frac{1.45T_C}{\Theta_D}\right)(1 - 0.62\mu^*)} \quad (6)$$

The EPC constant λ_{ep} is estimated to be 0.65, assuming the Coulomb pseudopotential $\mu^*=0.1$, which supports the weakly coupling scenario. The determined superconducting parameters of CaSn₃ single crystal are listed in Table I.

Figure 4 shows the calculated electronic structure of CaSn₃ based on the density functional theory calculations. Figure 4(a) presents the band structure in the vicinity of Fermi energy (E_F). According to the calculated band structure, CaSn₃ is a three-dimensional (3D) metal. The bands

near E_F are predominately contributed by p electrons of Sn ions (Fig. 4 (b)). Three bands with large dispersion cross the Fermi level, forming the complex 3D Fermi surfaces (shown in Figs. 4 (c)-(e)). From the calculated DOS (Fig. 4 (b)), one can notice that E_F locates at a valley of DOS, leading to a small $N(E_F)$ of 0.82 states/eV. The resulted $\gamma_{cal} = \frac{1}{3} \pi^2 k_B^2 N(E_F) = 1.93 \text{ mJ/mol K}^2$. Such value is lower than that of our measured CaSn_3 ($\gamma_{exp} = 2.9 \text{ mJ/mol K}^2$) obtained from the specific heat data. The enhancement of γ should be attributed to EPC with the factor of $\frac{\gamma_{exp}}{\gamma_{cal}} = 1 + \lambda_{ep}$, where λ_{ep} is derived to be ~ 0.5 , which is qualitatively in agreement with the weakly coupling scenario proposed above.

In order to understand the superconductivity of CaSn_3 single crystal, herein, we compare CaSn_3 superconductor with other AuCu_3 type alloys. As we know, researchers usually want to find a general rule to guide the exploration of the superconductors with higher T_C in the AuCu_3 type alloys. For example, the oscillation of T_C with respect to numbers of valence electrons n was suggested.[3, 13] On the other hand, a recent study shows that T_C monotonically increases with when the lattice constant a decrease for AX_3 ($A=\text{Y, La}$; $X=\text{Sn, Pb}$) compounds in AuCu_3 structure.[6] However, we found those rules are be applied to other AuCu_3 -type alloys. For example, our present CaSn_3 single crystal has smaller lattice parameter a but much lower T_C than that of LaSn_3 ($T_C \sim 6.5 \text{ K}$).[4] Moreover, the oscillation of T_C with respect to numbers of valence electrons n seems to be only effective for the AX_3 alloys in which the X atoms are from the same period.[3] Therefore, we should reconsider the superconductivity in AX_3 (X is metal elements in IV_A group) with AuCu_3 structure. Figure 5 shows the calculated DOS for the reported ASn_3 and APb_3 ($A=\text{Ca, Y, and La}$) compounds, which are of good agreement with previous reports.[27] The shapes of DOS curves near E_F for ASn_3 ($A=\text{Ca, Y, and La}$) are very similar except for the E_F that decided by the number of valence electrons n . YSn_3 and LaSn_3 , which can be seen as one electron doped CaSn_3 , have higher E_F locates at a small DOS peak (Fig. 5 (a)). Due to the large atomic number of Pb ion, the spin-orbit coupling is considered in the calculation of APb_3 . One can notice that the spin-orbit coupling makes the peaks of DOS sharper (Fig. 5 (b)).

We summarize the $N(E_F)$, lattice parameter a , and T_C of the reported ASn_3 and APb_3 ($A=\text{Ca, Y, La}$) superconductors in Fig. 6. The simple monotonic relationships between T_C and the lattice

parameter a or numbers of valence electrons n cannot be obtained. As we known, the EPC strength λ_{ep} for a material can be qualitatively expressed as:

$$\lambda_{ep} = \sum_{\alpha} \frac{\langle I_{\alpha}^2 \rangle N_{\alpha}(E_F)}{M_{\alpha} \langle \omega_{\alpha}^2 \rangle} \quad , \quad (7)$$

where the $\langle I_{\alpha}^2 \rangle$, M_{α} , and $\langle \omega_{\alpha}^2 \rangle$ are the mean square EPC matrix element averaged over Fermi surface, atomic mass, and averaged squared phonon frequency of the α th atom in the unit cell, respectively.[29] Since the $N(E_F)$ of AX_3 ($X=\text{Sn}$ and Pb) is predominately contributed by X , we can qualitatively propose that the total EPC is mainly decided by

$$\lambda_x = \frac{\langle I_x^2 \rangle N(E_F)}{M_x \langle \omega_x^2 \rangle} \quad , \quad (8)$$

where $X=\text{Sn}$ and Pb . Therefore, though La has a much larger atomic mass, when X is fixed, the T_C differences between YX_3 and $\text{La}X_3$ are small (less than 1 K), since the $N(E_F)$ of those two are close. Meanwhile, when X is fixed, YX_3 and $\text{La}X_3$ have higher $N(E_F)$ than that of $\text{Ca}X_3$, which leads to a higher T_C of YX_3 and $\text{La}X_3$. On the other hand, when X is changed from Sn to Pb , the EPC was strongly suppressed by the large increase of mass in the denominator of Eq. (8). For example, YPb_3 and LaPb_3 have the $N(E_F)$ three times larger than that of CaSn_3 . However, the T_C of the three compounds are on the same level (~ 4 K). The $N(E_F)$ of CaPb_3 is 50% higher than that of CaSn_3 . However, the T_C of CaPb_3 ($T_C \sim 1$ K) is only one fourth of that of CaSn_3 . According to the above analysis we can choose the suitable doping elements to increase $N(E_F)$ or decrease the mass of X atom to enhance the EPC and hence increase T_C . Moreover, compared to other cubic superconductors, such as MgCNi_3 ($T_C \sim 7$ K) with $N(E_F)$ of ~ 5 states/eV [30] and La_3Al ($T_C \sim 6$ K) with $N(E_F)$ of ~ 4 states/eV[31], CaSn_3 with superconductivity at the liquid helium temperature has a very small $N(E_F)$, which is unexpected. This indicates a large $\langle I^2 \rangle$ in the system. If AX_3 compounds with a lighter X atom in IV_A group (i.e., AGe_3 , ASi_3) can be obtained, the superconductivity with a much higher T_C might probably be achieved.

IV. Conclusion

In summary, we have investigated the physical properties of CaSn_3 single crystals. The electrical resistivity, magnetic susceptibility, and specific heat confirm that the superconductivity transition temperature of CaSn_3 is 4.2 K. Both $\Delta C_e/\gamma_N T_C$ and λ_{ep} value magnitudes indicate that the CaSn_3 is a weakly coupled superconductor. Furthermore, electronic band structure calculations are

consistent with experimental data and show the complex and multi-sheet Fermi surfaces. Based on the analysis of electron phonon coupling of AX_3 compounds ($A=Ca, La, \text{ and } Y; X=Sn, Pb$), we theoretically concluded a way to increase T_C in the system.

Acknowledgments

This work was supported by the Joint Funds of the National Natural Science Foundation of China and the Chinese Academy of Sciences' Large-Scale Scientific Facility under contracts (U1432139, U1232139), the National Nature Science Foundation of China under contracts (11304320, 51171177), the National Key Basic Research under contract 2011CBA00111, and the National Nature Science Foundation of Anhui Province under contract 1508085ME103. The authors thank Dr. Chen Sun for her assistance in editing the manuscript.

References:

- [1] E. Svanidze, L. Liu, B. Frandsen, B. D. White, T. Besara, T. Goko, T. Medina, T. J. S. Munsie, G. M. Luke, D. Zheng, C. Q. Jin, T. Siegrist, M. B. Maple, Y. J. Uemura, and E. Morosan, *Phys. Rev. X* **5**, 011026 (2015).
- [2] E. Svanidze and E. Morosan, *Phys. Rev. B* **85**, 174514 (2012).
- [3] Akira Iyo, Yousuke Yanagi, Tatsuya Kinjo, Taichiro Nishio, Izumi Hase, Takashi Yanagisawa, Shigeyuki Ishida, hijiri Kito, Nao Takeshita, Kunihiko Oka, Yoshiyuki Yoshida, and Hiroshi Eisaki, *Sci. Rep.* **5**, 10089 (2015).
- [4] R. J. Gambino, N. R. Stemple, and A. M. Toxen, *J. Phys. Chem. Solids* **29**, 295 (1968).
- [5] I. Sakamoto, S. Ohara, I. Oguro, and S. Maruno, *Physica B* **230**, 286 (1997).
- [6] K. Kawashima, M. Maruyama, M. Fukuma, and J. Akimitsu, *Phys. Rev. B* **82**, 094517 (2010).
- [7] R. Settai, K. Sugiyama, A. Yamaguchi, S. Araki, K. Miyake, T. Takeuchi, K. Kindo, Y. Onuki, and Z. Kletowski, *J. Phys. Soc. Jpn.* **69**, 3983 (2000).
- [8] A. P. Murani, *Phys. Rev. B* **28**, 2308 (1983).
- [9] T. F. Fässler and C. Kronseder, *Angew. Chem. Int. Ed. Engl.* **36**, 2683 (1997).

-
- [10] T. F. Fässler and S. Hoffmann, *Z. Anorg. Allg. Chem.* 626, 106 (2000).
- [11] J.C.P. Klaasse, R. T. W. Meijer, and F.R. de Boer, *Solid State Commun.* 33, 1001 (1980).
- [12] A. E. Baranovskiy, G. E. Grechnev, and I. V. Svechkarev, *Low Temp. Phys.* 32, 849 (2006).
- [13] E. E. Havinga, H. Damsma, and M. H. Van Maasen, *J. Phys. Chem. Solids* 31, 2652 (1970).
- [14] J. P. Perdew, K. Burke, and M. Ernzerhof, *Phys. Rev. Lett.* 77, 3865 (1996).
- [15] P. Giannozzi, et al., *J. Phys.: Condens. Matter* 21, 395502 (2009).
- [16] K.F. Garrity, J.W. Bennett, K.M. Rabe, and D. Vanderbilt, *Comput. Mater. Sci.* 81, 446 (2014).
- [17] H. J. Monkhorst and J. D. Pack, *Phys. Rev. B* 13, 5188 (1976).
- [18] F. J. Blatt, *Physics of Electronic Conduction in Solids* (McGraw-Hill, New York, 1968).
- [19] Mott, N. F; Jones, H. *The Theory of the Properties of Metals and Alloys*; Oxford University Press: London, U.K., 1958.
- [20] N. R. Werthamer, E. Helfand, and P. C. Hohenberg, *Phys. Rev.* 147, 295 (1966).
- [21] A. M. Clogston, *Phys. Rev. Lett.* 9, 266 (1962).
- [22] Neel Haldolaarachchige, Quinn Gibson, Jason Krizan, and R. J. Cave, *Phys. Rev. B* 89, 104520 (2014).
- [23] D. Hirai, M. N. Ali, and R. J. Cava, *J. Phys. Soc. Jpn.* 82, 124701 (2013).
- [24] A. B. Karki, D. A. Browne, S. Stadler, J. Li, and R. Jin, *J. Phys.: Condens. Matter* 24, 055701 (2012).
- [25] P. B. Allen and R. C. Dynes, *Phys. Rev. B* 12, 905 (1975).
- [26] H. Padamsee, J. E. Neighbor, and C. A. Shiffman, *J. Low Temp. Phys.* 12, 387 (1973).
- [27] W. L. McMillan, *Phys. Rev.* 167, 331 (1968).
- [28] Swetarekha Ram, V. Kanchana, A. Svane, S. B. Dugdale, and N. E. Christensen, *J. Phys.: Condens. Matter* 25, 155501 (2013).
- [29] L. N. Cooper, *Phys. Rev.* 104, 1189 (1956); J. Bardeen, L. N. Cooper, and J. R. Schrieffer, *Phys. Rev.* 106, 162 (1957); J. Bardeen, L. N. Cooper, and J. R. Schrieffer, *Phys. Rev.* 108, 1175 (1957).
- [30] D. J. Singh and I. I. Mazin, *Phys. Rev. B* 64, 140507(R) (2001).
- [31] P. Ravindran and R. Asokaman, *J. Phys.: Condens. Matter* 7, 5567 (1995).

Table I: Superconducting parameters of CaSn₃ single crystal.

Parameters	Units	CaSn ₃
T_C	K	4.2
ρ_0	$\mu \Omega cm$	1.3
A	$\mu \Omega cm/K^2$	$2.27 \cdot 10^{-3}$
RRR		73
$\mu_0 H_{C1}(0)$	Oe	125
$\mu_0 H_{C2}(0)$	T	1.79
$\mu_0 H_C(0)$	T	0.15
$\mu_0 H^{pauli}$	T	7.6
$\xi(0)$	\AA	136
$\lambda(0)$	\AA	1147
$\kappa(0)$		8.44
$\gamma(0)$	$\frac{mJ}{mol K^2}$	2.9
β	$\frac{mJ}{mol K^4}$	1.45
$\frac{\Delta C}{\gamma T_C}$		1.13
Θ_D	K	175
Θ_R	K	211
λ_{ep}		0.65

Figure captions:

Fig. 1 (Color online): (a) Cubic perovskite crystal structure of CaSn_3 ; (b) Powder XRD patterns at room temperature for the crushed CaSn_3 single crystals. The vertical red bars and blue ones stand for the position of Bragg peaks of CaSn_3 and Sn in PDF card, respectively. The inset presents the picture of CaSn_3 single crystal used for this study; (c) The temperature dependence of the resistivity of CaSn_3 single crystal. The red solid line is the fitting by using the Bloch-Grüneisen-Mott (BGM) model. Inset shows an enlarged view of the plot in a low temperature range ($T < 30$ K). The solid line is the fitting to the data using from Fermi-liquid model; (d) ZFC and FC magnetic susceptibility of CaSn_3 single crystal measured at $H=10$ Oe. Inset of (i) shows the temperature dependence of magnetization in a large scale; (ii) presents the magnetic field dependence of magnetization at $T=2.5$ K.

Fig. 2 (Color online): (a) Temperature dependence of $\rho(T)/\rho(5\text{ K})$ under magnetic field of 0, 500, 1000, 2000, 3000, 4000, and 5000 Oe from right to left, respectively; (b) The upper critical field $\mu_0 H_{C2}$ as a function of T_C . Solid lines are fits to Eq. (2) and (4), respectively; (c) The magnetic field dependence of magnetization at different temperatures; (d) The lower critical field $\mu_0 H_{C1}$ dependence of T_C . The solid line is fit to Eq. (3).

Fig. 3 (Color online): The main panel shows the heat capacity in 0 T and 5 T magnetic fields. The blue line shows the heat capacity data fitting with the equation $C_p/T = \gamma_N + \beta T^2$. The inset shows that the heat capacity jumps around T_C .

Fig. 4 (Color online): (a) Band structure of CaSn_3 . The bands crossing E_F are colored; (b) DOS of CaSn_3 ; (c), (d), and (e) are the Fermi surface from the bands colored with red, blue, and purple in (a), respectively.

Fig. 5 (Color online): DOS of (a) ASn_3 and (b) APb_3 for $A=\text{Ca}, \text{Y}, \text{and La}$.

Fig. 6 (Color online): Lattice parameter a dependence of T_C for the reported AX_3 (X is metal elements in IV_A group) superconductors (data from Ref. 13).

Figure 1:

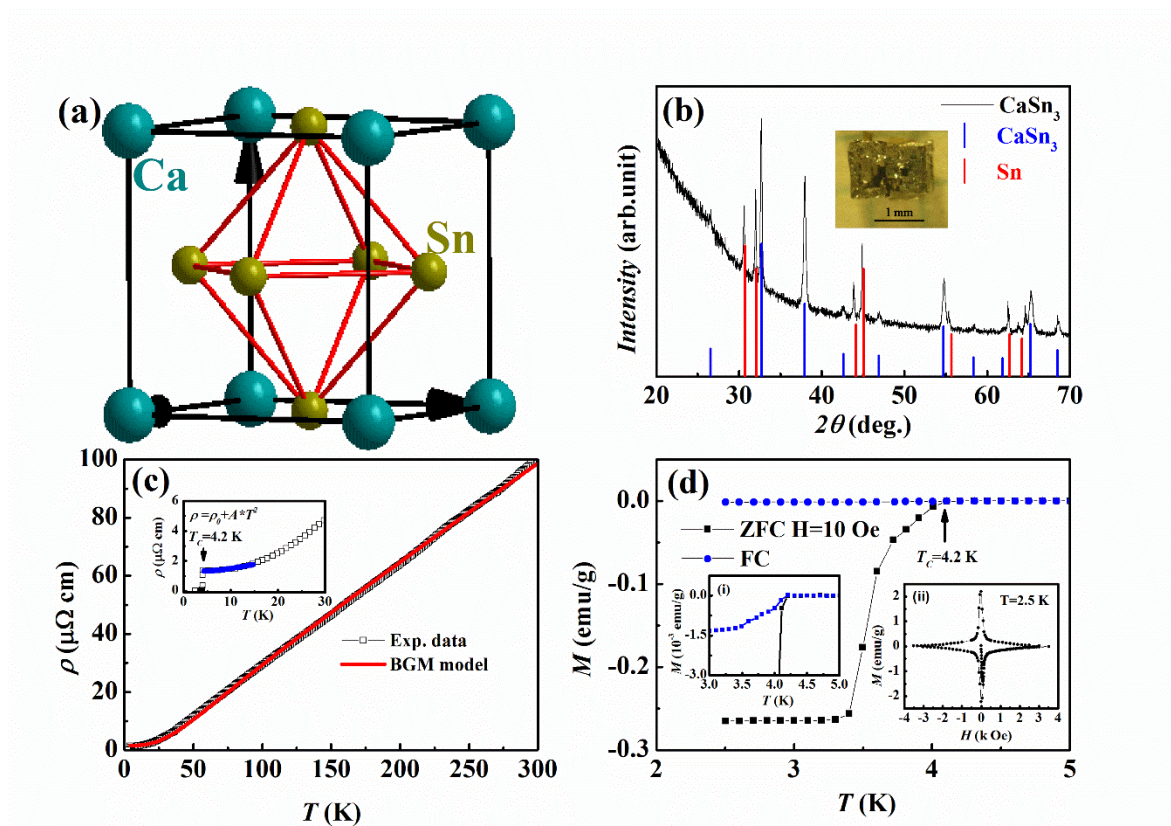


Fig. 1 X. Luo *et al.*

Figure 2:

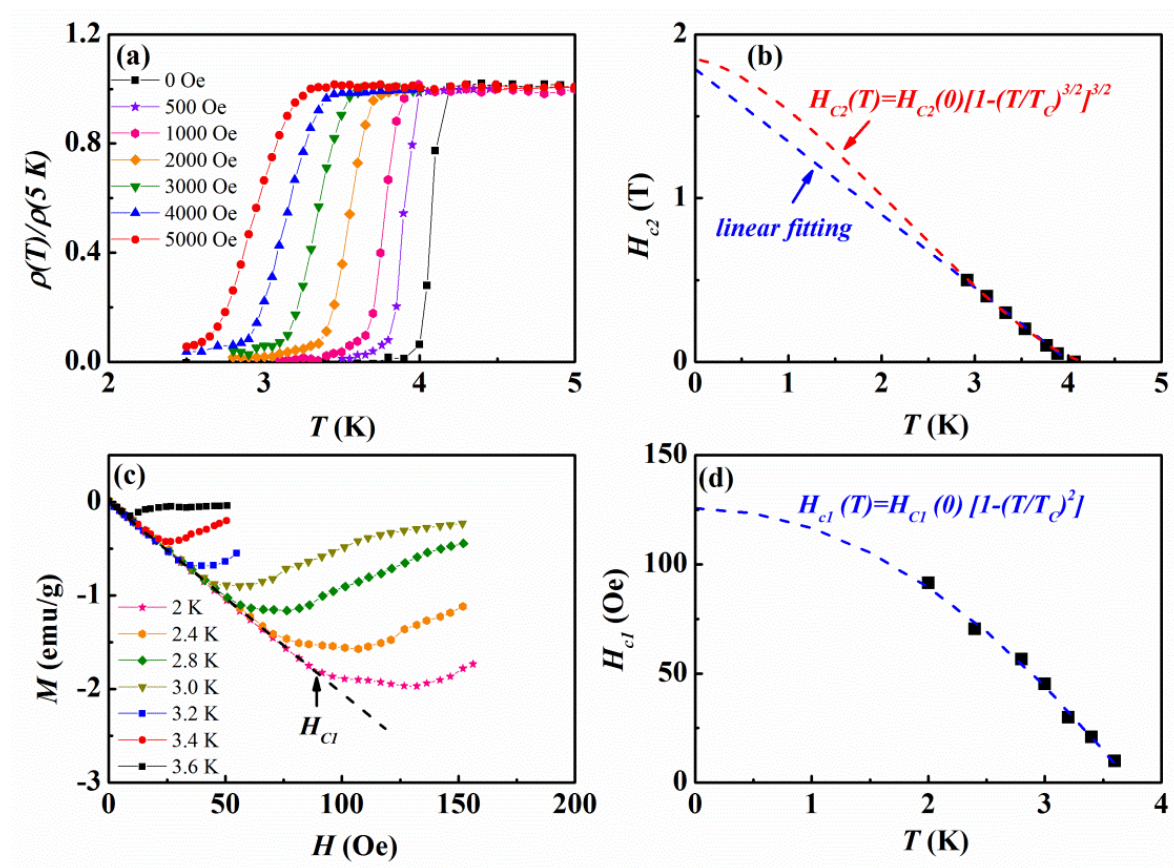


Fig.2 X. Luo et al.

Figure 3:

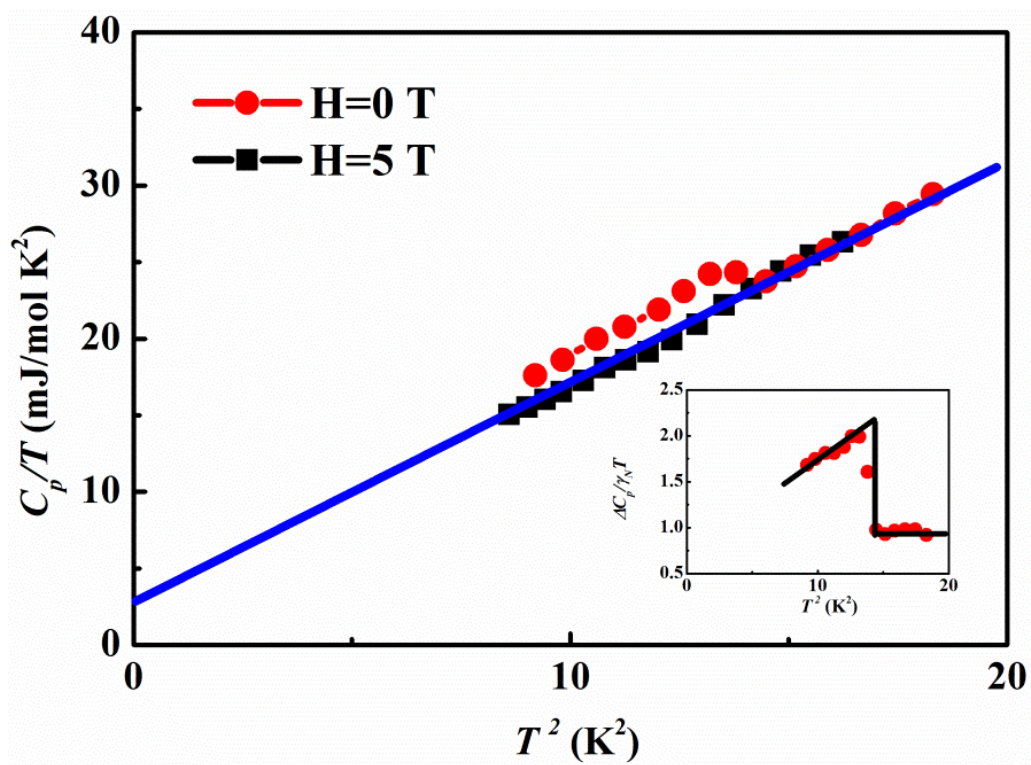


Fig. 3 X. Luo *et al.*

Figure 4:

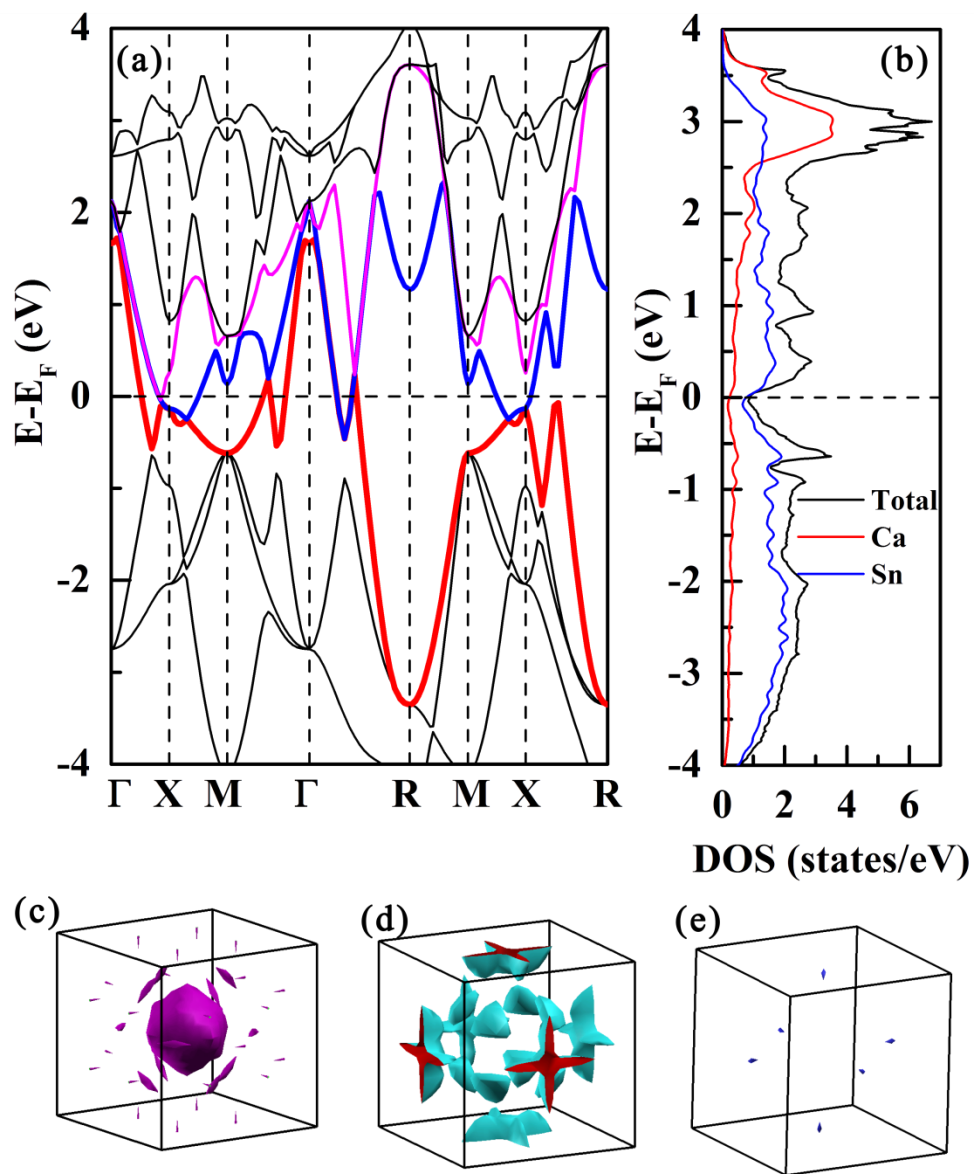


Fig.4 X. Luo *et al.*

Figure 5:

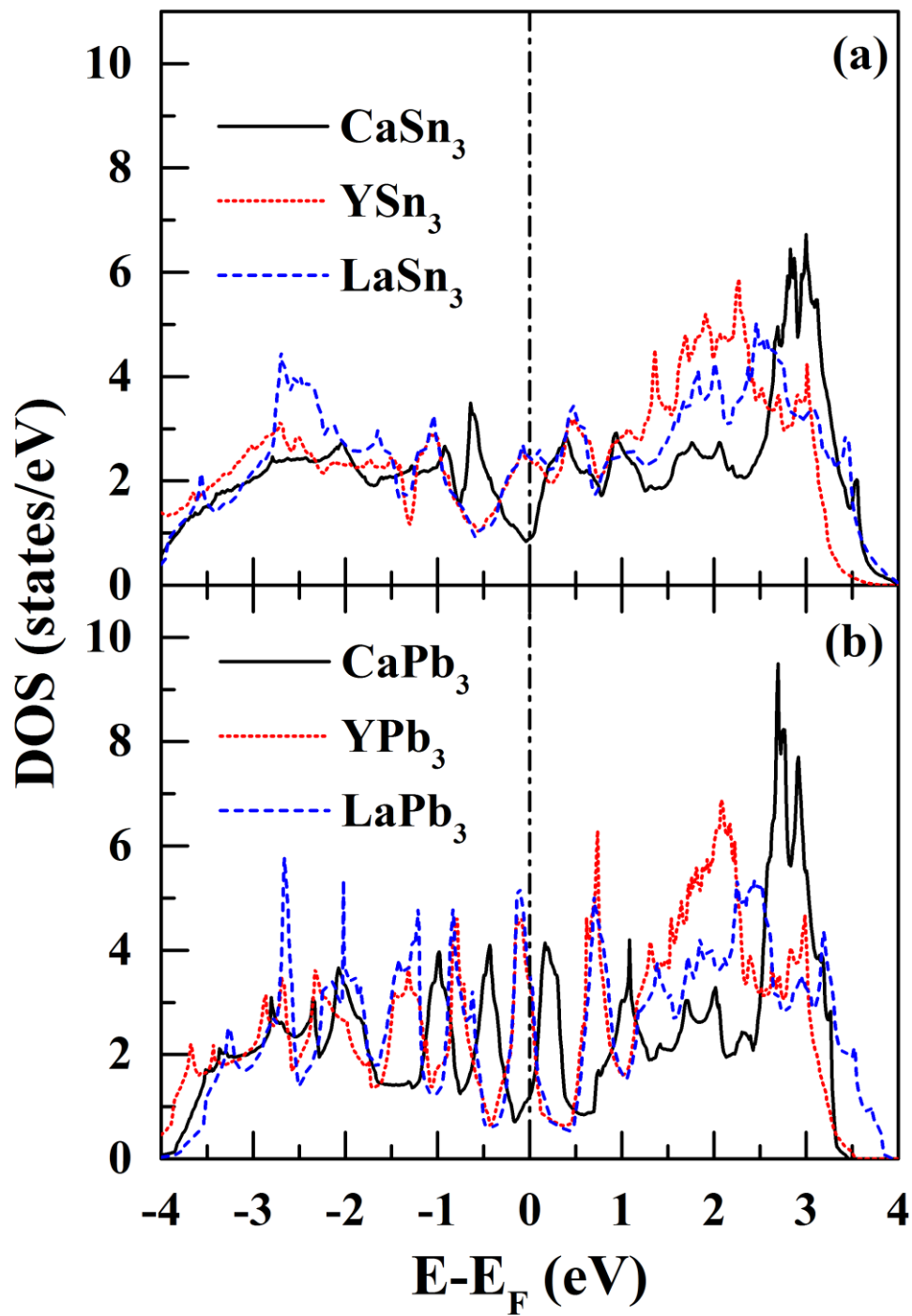


Fig.5 X. Luo *et al.*

Figure 6:

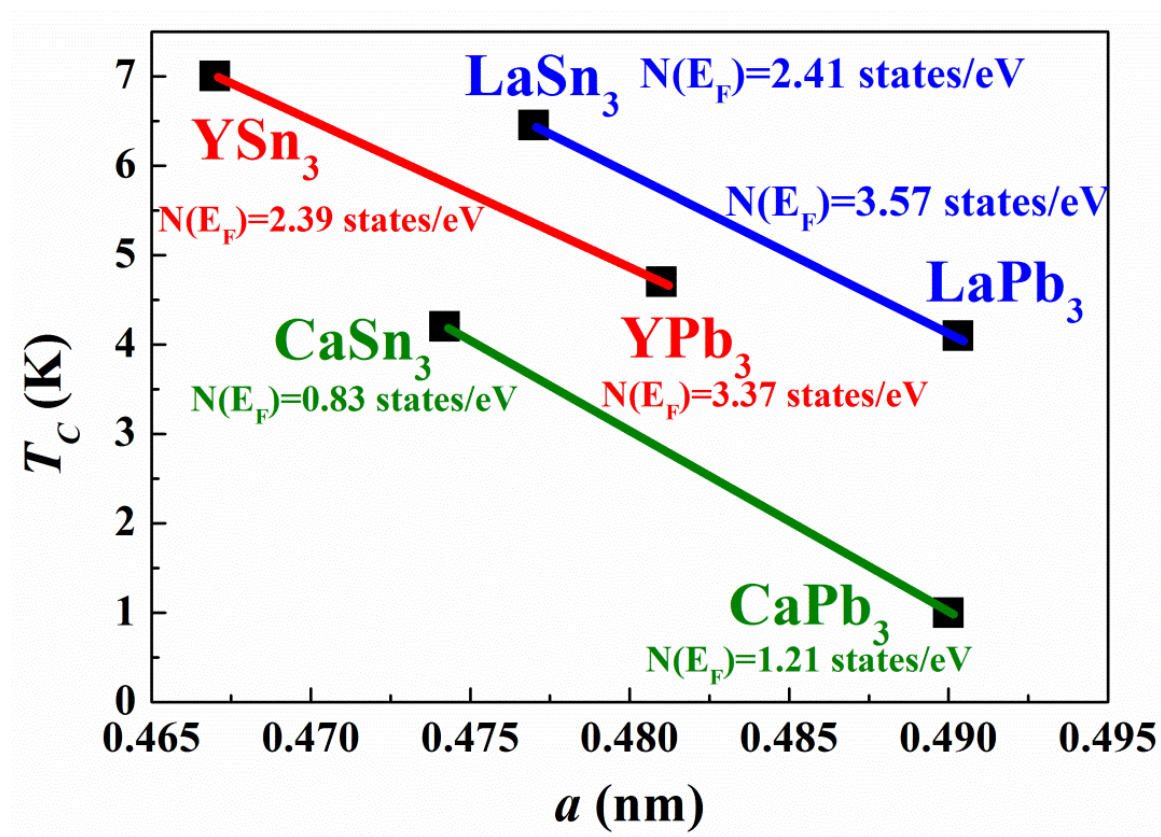


Fig. 6 X. Luo *et al.*

Supporting Information

Superconductivity in CaSn₃ single crystal with a AuCu₃-type structure

X. Luo^{1†}, D. F. Shao^{1†}, Q. L. Pei¹, J. Y. Song¹, L. Hu¹, Y. Y. Han², X. B. Zhu¹, W. H. Song¹,

W. J. Lu^{1*} and Y. P. Sun^{1,2,3*}

¹ Key Laboratory of Materials Physics, Institute of Solid State Physics, Chinese Academy of Sciences, Hefei, 230031, China

² High Magnetic Field Laboratory, Chinese Academy of Sciences, Hefei, 230031, China

³ Collaborative Innovation Center of Advanced Microstructures, Nanjing University, Nanjing, 210093, China

Abstract

We report the superconductivity of the CaSn₃ single crystal with a AuCu₃-type structure, namely cubic space group $P_{m\bar{3}m}$. The superconducting transition temperature $T_C=4.2$ K is determined by the magnetic susceptibility, electrical resistivity, and heat capacity measurements. The magnetization versus magnetic field (M - H) curve at low temperatures shows the typical-II superconducting behavior. The estimated lower and upper critical fields are about 125 Oe and 1.79 T, respectively. The penetration depth $\lambda(0)$ and coherence length $\xi(0)$ are calculated to be approximately 1147 nm and 136 nm by the Ginzburg-Landau equations. The estimated Sommerfeld coefficient of the normal state γ_N is about 2.9 mJ/mol K². $\Delta C/\gamma_N T_C=1.13$ and $\lambda_{ep}=0.65$ suggest that CaSn₃ single crystal is a weakly coupled superconductor. Electronic band structure calculations show a complex multi-sheet Fermi surface formed by three bands and a low density of states (DOS) at the Fermi level, which is consistent with the experimental results. Based on the analysis of electron phonon coupling of AX₃ compounds (A=Ca, La, and Y; X=Sn and Pb), we theoretically proposed a way to increase T_C in the system.

Electronic mail: wjlu@issp.ac.cn and ypsun@issp.ac.cn

More experimental details:

The used crystals were cubic or rectangle shape, we decanted the crystals is about 270 °C, which is higher than the melting point of element Sn (231 °C) and decanting speed is very fast and can reach 1800 round/second within 10 seconds. We did the polishing before doing the measurements, so just little element Sn may be left on the surface.

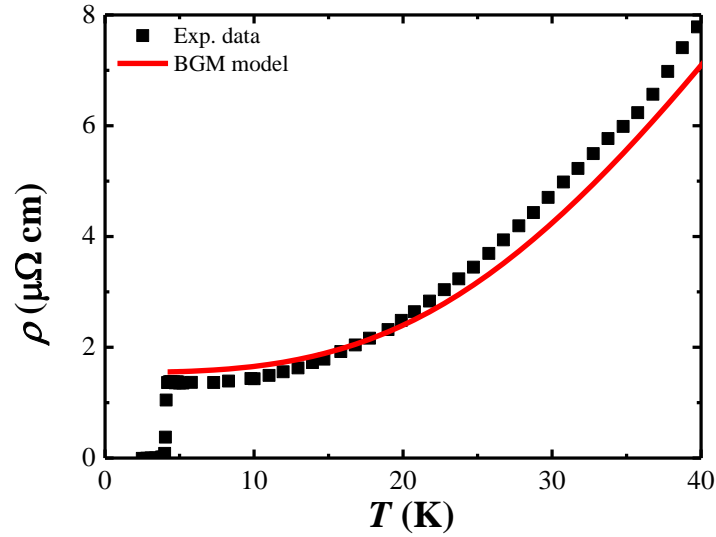
Figures:

Fig. S1: The fitting result using the BGM model is shown at the low temperature.

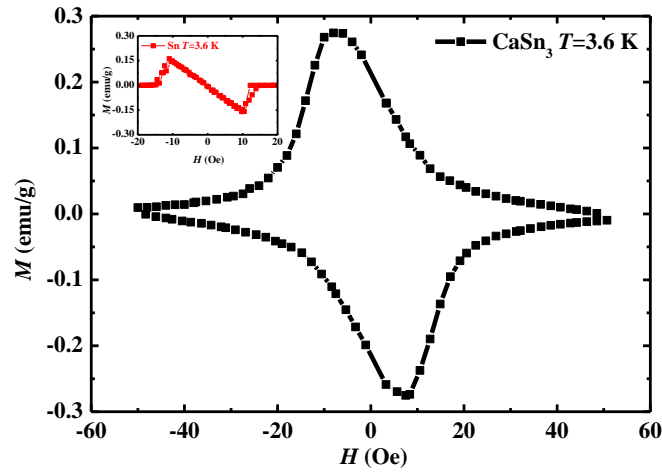


Fig. S2: The comparison of $M(H)$ between the CaSn_3 single crystal and element Sn at $T=3.6$ K.